Dynamic Light Scattering of Poly(vinyl alcohol) Solutions and Their Dynamical Behavior during the Chemical Gelation Process

Anna-Lena Kjøniksen and Bo Nyström*

Department of Chemistry, University of Oslo, P.O. Box 1033, Blindern, N-0315 Oslo, Norway

Received May 14, 1996; Revised Manuscript Received August 15, 1996[⊗]

ABSTRACT: Dynamic light scattering experiments have been carried out on semidilute aqueous solutions of poly(vinyl alcohol) (PVA) and on gelling PVA solutions in the presence of a constant amount of cross-linker agent. The time correlation data revealed, for all the solutions and the systems in the pregel domain, the existence of two relaxation modes. The "fast" mode (exhibits an almost exponential profile) was always diffusive. In the solutions, the "slow" mode (described by a stretched exponential) was diffusive at high concentrations and a somewhat stronger wave vector (**q**) dependence was observed at lower concentrations. The concentration dependence of the slow relaxation time (τ_s) could be described by a power law ($\tau_s \sim c^4$). In the pregel domain, the slow mode was diffusive for systems of high polymer concentration, while for systems of low concentration, a much stronger **q** dependence was detected when the gelation threshold was approached. The cooperative diffusion coefficient (D_c), evaluated from the "fast" mode, decreased for systems of low polymer concentration as the gelation process proceeded, while for systems of higher concentration, D_c was practically constant in the whole pregel zone. These results suggest that incipient gels formed from systems of low polymer concentration are more heterogeneous than their corresponding solutions, while in systems of higher polymer concentration, the nonuniformities of the network are practically the same for the solution and the corresponding incipient gel. Close to the gelation threshold, the slow mode could be described by a power law. In the postgel regime, the slow mode was absent and the decay of the correlation function could be approximated by a single exponential. Incipient gels and gels in the postgel zone exhibited nonergodic features.

Introduction

In recent years much effort has been devoted to the study of structure and dynamics of aqueous poly(vinyl alcohol) (PVA) solutions and their corresponding gels.[1−6] Dynamic light scattering studies on related systems, namely, on associating aqueous solutions of PVA−borax[7,8] and PVA−Congo red,[9] have recently been reported. The gel systems exhibit superstructures[10] on variable-length scales that depend on the conditions of preparation, e.g., the cross-linking density, the polymer concentration, pH, and the time of storage of the sample. In aqueous solutions, clustering of chains is caused primarily by association between the polar groups of the dissolved polymer. In previous studies of structural[2−5] and dynamic[3,4,11] properties of PVA systems, most of the attention has been focused on the comparison of chemically cross-linked PVA hydrogels and their corresponding semidilute polymer solutions. These results revealed[3,5] the presence of large-scale static nonuniformities in both the solutions and the gels, and the amount of static nonuniformities strongly increased with the cross-linking density. However, there is a lack of investigations dealing with the dynamical features of semidilute solutions of PVA and their dynamical behaviors during the chemical gelation process.

This paper presents dynamic light scattering (DLS) results on PVA solutions in the semidilute regime and on the same solutions in the presence of a constant amount of cross-linker (9 mM glutaraldehyde). This low concentration of cross-linking agent yields low cross-linking densities and only weakly cross-linked gels are formed. The DLS measurements are carried out at different scattering angles, and the association behavior during the gelation process is monitored. The DLS results for solutions and systems in the pregel domain reveal the existence of a "slow" relaxation mode, which can be described by a stretched exponential. The features of this mode depend on inter alia the polymer concentration and on the stage of gelation. The results from this study indicate that the polymer concentration affects the heterogeneity of the network. The aim of this work is to gain further insight into the complex dynamics operating in associating polymer systems.

Experimental Section

Materials and Solution Preparation. A commercial poly(vinyl alcohol) sample, having a molecular weight of M_v = 53 000 (determined from viscosity measurements), was obtained from Hoechst AG and used as received. The polydispersity of the polymer is ∼2, and the degree of saponification is 99 mol %. Semidilute PVA solutions in the range 2−6% (w/w) were prepared by weighing the components, and PVA was dissolved in distilled water at ∼90 °C, followed by stirring for some hours. The pH of the solutions was adjusted to 2.4 by adding small amounts of HCl(aq) to the solutions. DLS experiments were also performed on solutions where a small amount of glutaraldehyde (GA) had been added to the solutions under vigorous stirring. The concentration of the cross-linking agent was always 9 mM, yielding low cross-linking densities.

Dynamic Light Scattering. The beam from an argon ion laser (Spectra Physics Model 2020), operating at the wavelength 514.5 nm with vertically polarized light, was focused on the sample cell through a temperature-controlled chamber (the temperature constancy being controlled to within ±0.05 °C) filled with refractive index matching silicone oil. The sample solutions were filtered in an atmosphere of filtered air through, depending on the viscosity of the solution, 0.22- or 0.45-μm filters (Millipore) directly into precleaned 10-mm NMR tubes (Wilmad Glass Co.) of highest quality.

The light-scattering process defines a wave vector $\mathbf{q} = (4\pi n/\lambda)\sin(\theta/2)$, where λ is the wavelength of the incident light in a vacuum, θ is the scattering angle, and n is the refractive index of the medium. The value of n was determined for each solution at λ = 514.5 nm by using an Abbe' refractometer. All measurements were carried out at 25 °C.

The full homodyne intensity autocorrelation function was measured at scattering angles in the range 30−90° with an

[⊗] Abstract published in *Advance ACS Abstracts,* October 1, 1996.

S0024-9297(96)00705-X CCC: $12.00

ALV-5000 multiple-τ digital correlator. The correlation functions were recorded in the real time "multiple-τ" mode of the correlator, in which 256 time channels are logarithmically spaced over an interval ranging from 0.2 μs to almost 1 h.

Analysis of the Dynamic Light Scattering Data. DLS is a powerful technique to probe dynamics, on different length and time scales, in systems of various complexities. When the scattered light obeys Gaussian statistics, the measured homodyne intensity autocorrelation $g^{(2)}(\mathbf{q},t)$ is related to the theoretically amenable first-order electric field correlation function $g^{(1)}(\mathbf{q},t)$ through the Siegert relation[12]

$$g^{(2)}(\mathbf{q},t) = 1 + B|g^{(1)}(\mathbf{q},t)|^2 \qquad (1)$$

where B (≤ 1) is the coherence factor that depends on the experimental geometry. In a DLS experiment, which probes how concentration fluctuations relax toward equilibrium at a length scale of $1/\mathbf{q}$, concentration fluctuations with well-defined wave vectors are monitored, and the time dependence of $g^{(1)}(\mathbf{q},t)$ is given by $g^{(1)}(\mathbf{q},t) = \langle \delta c_{\mathbf{q}}(t) \delta c_{-\mathbf{q}}(0) \rangle / \langle |\delta c_{\mathbf{q}}|^2 \rangle$, where $\delta c_{\mathbf{q}}(t)$ is the concentration fluctuation of wave vector $\mathbf{q}$.

Several experimental DLS studies[1,3,4,7−9,11−41] on complex polymer systems have revealed the existence of two relaxation modes. In this work, these modes both exhibit a nonexponential feature, and we have therefore fitted the correlation functions in this study to a double Kohlrausch−Williams−Watts (KWW)[42,43]-stretched exponential function given by

$$g^{(1)}(t) = A_f \exp[-(t/\tau_{fe})^{\gamma}] + A_s \exp[-(t/\tau_{se})^{\beta}] \qquad (2)$$

with $A_f + A_s = 1$. The parameters A_f and A_s are the amplitudes for the fast and the slow relaxation modes, respectively. Analyses of the time correlation functions of the concentration fluctuations at long wavelengths in the semidilute concentration regime have shown that the first term (short-time behavior) on the right-hand side of eq 2 is related to a cooperative diffusion coefficient D_c ($\tau_f^{-1} = D_c \mathbf{q}^2$), which reflects a concerted motion of polymer chains relative to the solvent. The conjecture is that the second term (long-time behavior) is associated with disengagement relaxation of individual chains or cluster relaxation.[16,29] The variables τ_{fe} and τ_{se} are some effective relaxation times, and γ ($0 < \gamma \leq 1$) and β ($0 < \beta \leq 1$) measure the widths of the distributions of relaxation times. The mean relaxation times are given by

$$\tau_f \equiv \int_0^{\infty} \exp[-(t/\tau_{fe})^{\gamma}]\, dt = (\tau_{fe}/\gamma)\Gamma(1/\gamma) \qquad (3a)$$

$$\tau_s \equiv \int_0^{\infty} \exp[-(t/\tau_{se})^{\beta}]\, dt = (\tau_{se}/\beta)\Gamma(1/\beta) \qquad (3b)$$

where Γ is the gamma function.

In the analysis of the correlation function data, a nonlinear fitting algorithm (a modified Levenberg−Marquardt method) was used to obtain best-fit values of the parameters A_f, τ_{fe}, γ, τ_{se}, and β appearing on the right-hand side of eq 2. The values of γ determined in this study were always close to 1 ($\gamma \approx 0.9$), but in order to account for polydispersity effects, this parameter was allowed to float in the fitting process. In previous DLS studies[13,16,20,29,33,36] the value of γ has often been observed to be close to 1, and therefore, the fast mode has been approximated by a single exponential.

Results and Discussion

Semidilute PVA Solutions. Figure 1 shows time correlation function data at scattering angles of 90 (a) and 30° (b) for different concentrations of PVA, together with the corresponding curves fitted with the aid of eq 2. The insets in Figure 1 show semilogarithmic plots of $g^1(t)$ as a function of t^{β} for the concentrations indicated. This type of plot yields straight lines for functions that can be represented by stretched exponentials. We observe that, within experimental error, the long-time behaviors of the correlation functions at all conditions are well described by straight lines. We have found that the time correlation functions of PVA solutions and of gelling PVA systems in the pregel domain can always be described by a double sum of stretched exponentials. We note that, at both scattering angles, there is a progessive slowing down of the long-time relaxation process as the polymer concentration increases. A characteristic feature of the decays at both scattering angles is the gradual formation at higher concentrations of a "plateaulike" domain, which is visible in the correlation function data at intermediate times. This behavior indicates the formation of large clusters,[15,21,33] and the plateaulike region is usually more pronounced at low scattering angles. These features are consistent with recent static light scattering and small-angle neutron scattering studies[3,4,11] on PVA solutions and gels, where the excess scattered intensity observed at low $\mathbf{q}$ values was attributed to the clustering of PVA molecules in aqueous solutions.

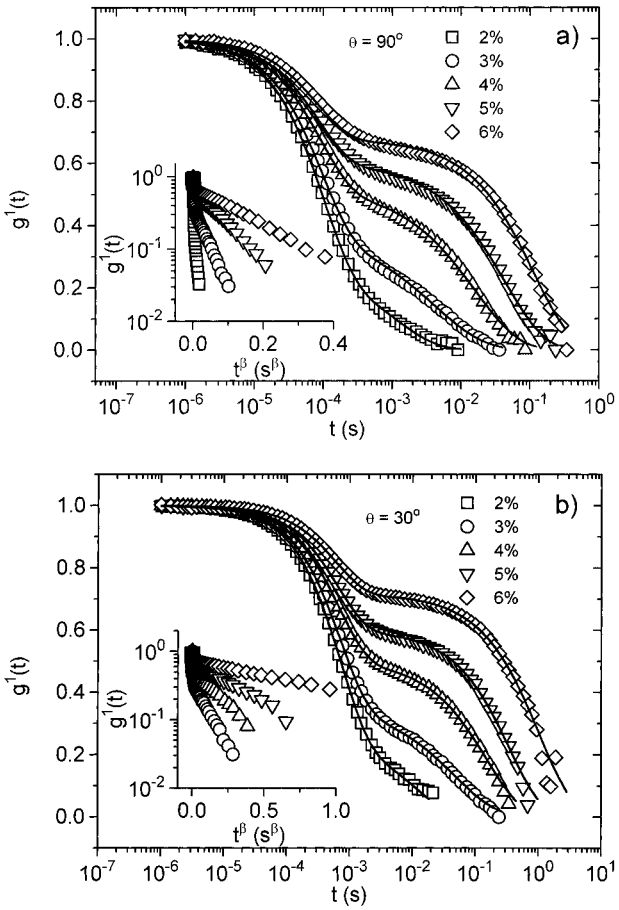

Figure 1. First-order electric field correlation function versus time (every second data point is shown) for solutions of PVA at the concentrations and scattering angles indicated. The curves are fitted with the aid of eq 2. The inset plots demonstrate the stretched exponential character of the correlation functions at long time.

By using the model equation (see eqs 2 and 3), a number of characteristic parameters can be extracted. Let us first discuss the effects of scattering angle on the relaxation modes. Figure 2a−c shows the angular dependences of the time correlation functions at different concentrations. These results clearly show the evolution of a plateaulike domain at higher concentrations. The inset plots illustrate the $\mathbf{q}$ dependences of the correlation functions, at different concentrations, in a reduced form. We can see that the correlation function data at different scattering angles practically

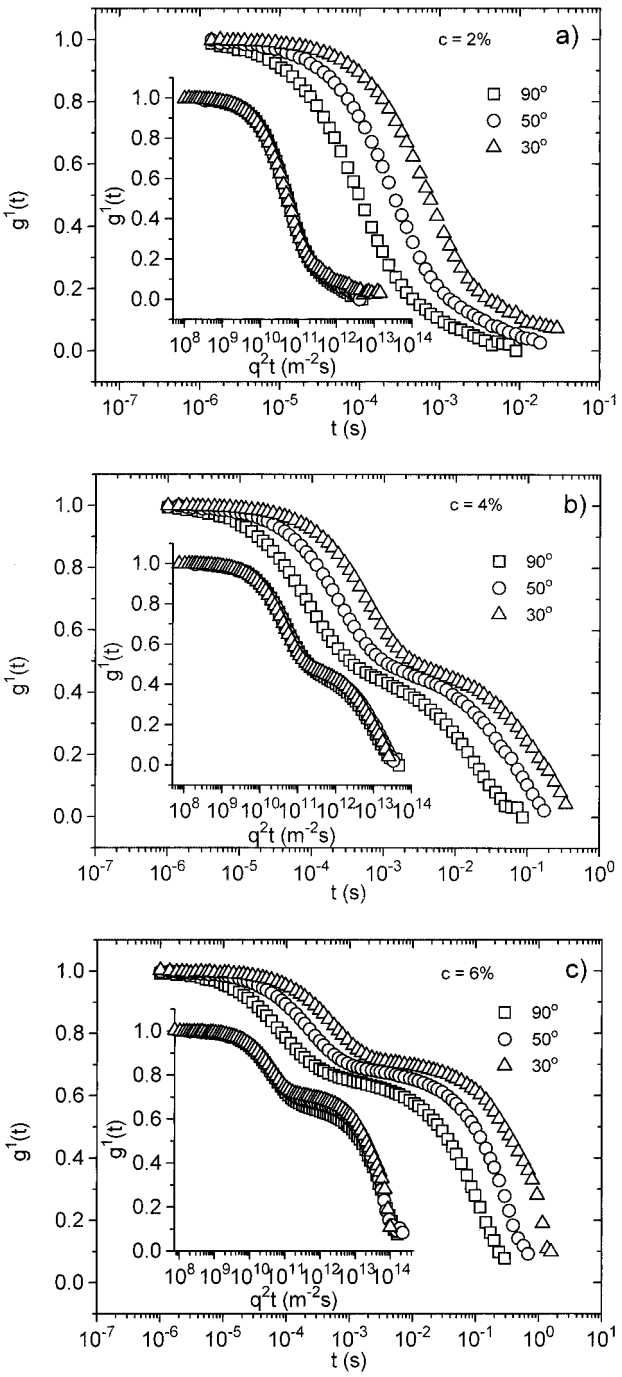

Figure 2. First-order electric field correlation function versus time (every second data point is shown) for solutions of PVA at the concentrations and scattering angles indicated. The inset plots show the same correlation functions versus $\mathbf{q}^2t$.

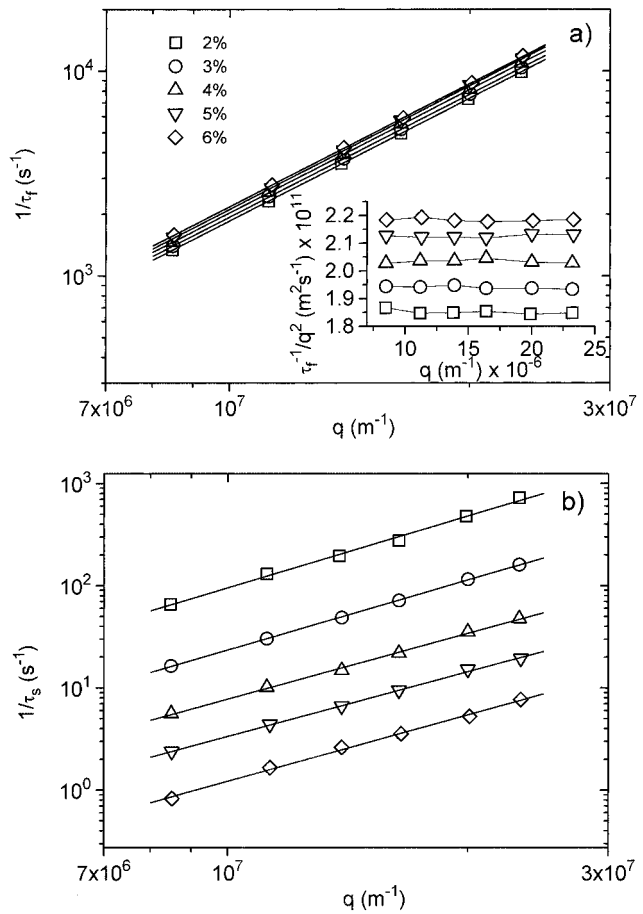

Figure 3. Inverse relaxation times as a function of wave vector for solutions of PVA at the concentrations indicated. (a) τ_f^{-1} versus $\mathbf{q}$; (b) τ_s^{-1} versus $\mathbf{q}$. The inset plot shows that the fast mode is diffusive.

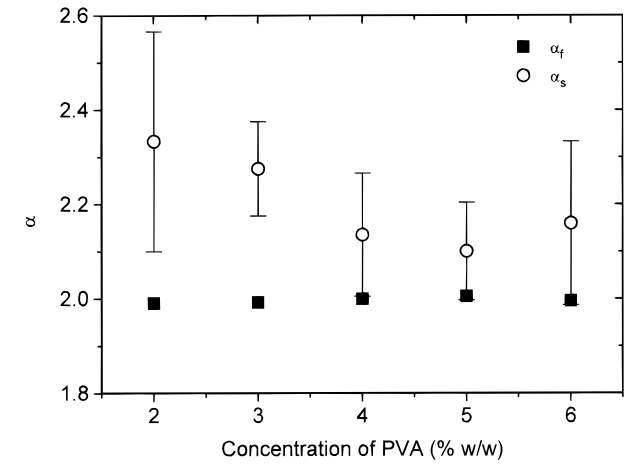

Figure 4. Power law exponent α, illustrating the **q** dependences of the inverse relaxation times as a function of concentration. The error bars represent three times the standard deviation.

collapse onto a single curve for the concentrations of 4 and 6% (w/w) (see Figure 2b,c), reflecting the diffusive character of the relaxation modes. However, for the lowest concentration (2% w/w), a separation of the curves at longer times can be traced, suggesting a stronger q dependence of the "slow" relaxation process.

The **q** dependences of the inverse "fast" and "slow" relaxation times can be expressed as $\tau_f^{-1} \sim \mathbf{q}^{\alpha_f}$ and $\tau_s^{-1} \sim \mathbf{q}^{\alpha_s}$, respectively. In order to quantitatively determine the **q** dependences of the relaxation times (τ_f and τ_s), plots of the inverse relaxation times as a function of **q** are depicted in Figure 3. From the slopes of the straight lines the numerical values of the scaling law exponents, at different concentrations, are determined. The fast mode is always diffusive (see the inset plot of Figure 3a and Figure 4), while the slow mode exhibits a stronger **q** dependence at lower concentrations.

The value of α_f is independent of polymer concentration and assumes a value of 2 (see Figure 4), which is the hallmark of a diffusive process. The inverse slow relaxation time exhibits a somewhat stronger **q** dependence than that of a diffusive process at low concentrations. The slow mode may be interpreted as arising from the presence of large-scale heterogeneities. The surmise for the present system is that the strong

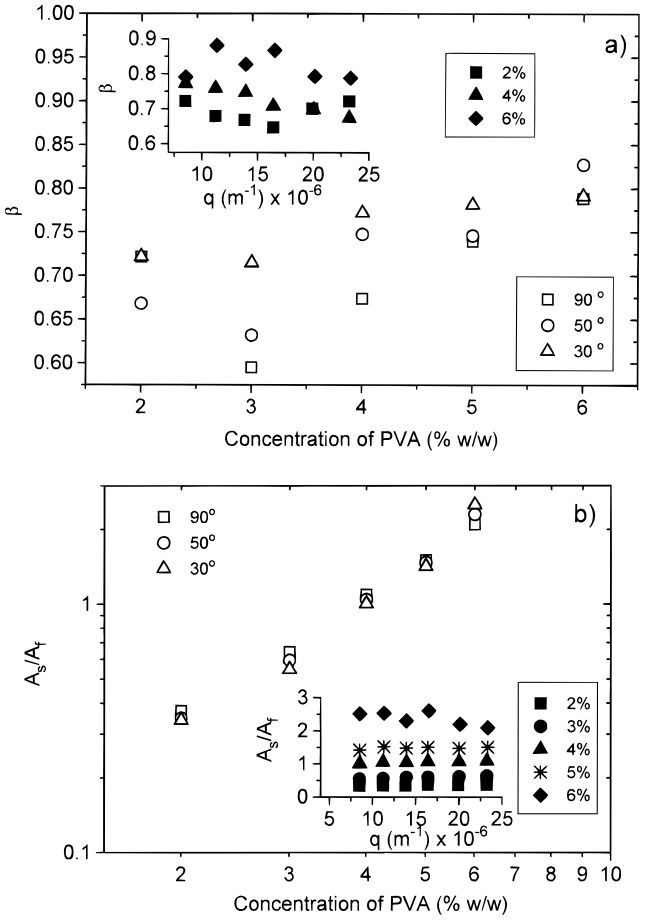

Figure 5. Concentration dependences of β (a) and A_s/A_f (b) for the scattering angles indicated. The inset plots show the **q** dependences of the quantities at the concentrations indicated.

intermolecular associations give rise to large heterogeneities in the incipient semidilute regime and the solution structure is characterized by a collection of many clusters of various sizes, which are slightly interconnected to each other. At this stage, the slow process corresponds to a translational diffusion of large clusters superimposed by many internal relaxation modes[15] of motion (giving rise to the augmented **q** dependence of the inverse slow relaxation time). At higher polymer concentrations, the heterogeneity of the network decreases and the slow relaxation process is characterized by the translational diffusion motion of clusters of macromolecules through the entangled polymer matrix.[1,44] This hypothesis of decreased heterogeneity with increasing concentration is favored by the results of the stretched exponent β in Figure 5a. Although the data are scattered, the general trend is that β increases with concentration. This indicates that the heterogeneities of the cluster size distribution become less with increasing concentration and a more homogeneous network is formed. In the inset plot of Figure 5a, we can trace a weak decrease of β with increasing scattering angle for all concentrations. An augmented **q** dependence of the slow mode ($\mathbf{q}^2 - \mathbf{q}^3$) has recently been reported[8] for aqueous borax solutions of PVA in the incipient semidilute range. A stronger **q** dependence of the slow mode, seems to be an usual feature of associating polymer systems of various natures.[16,20,23,29,30,45] This effect is usually attributed to the formation of large clusters.

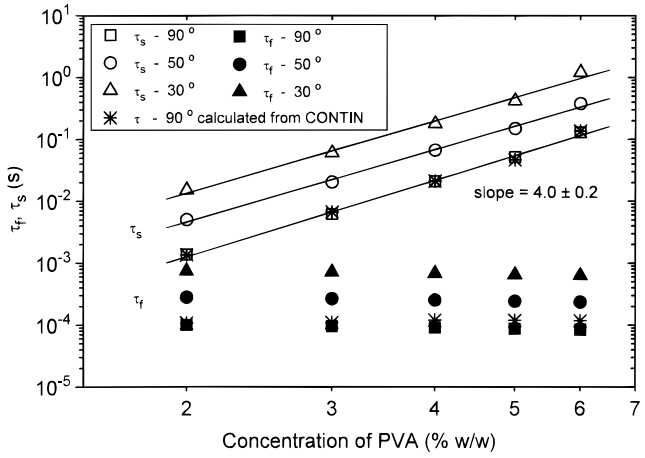

Figure 6. Concentration dependences of the slow and the fast relaxation times for solutions of PVA at the scattering angles indicated. Data calculated with the aid of CONTIN have also been included (see text for details).

The variation of the ratio A_s/A_f as a function of concentration is depicted in Figure 5b. The ratio increases strongly with concentration at all scattering angles, and the inset plot reveals no significant **q** dependence of the ratio. These results suggest that the slow mode becomes more dominant with increasing polymer concentration.

Figure 6 shows the concentration dependences of the relaxation times, calculated with the aid of eq 2 in combination with eq 3, at different scattering angles. The mean relaxation times calculated by the CONTIN method[46] have also been included in Figure 6. The agreement between these values and the corresponding ones determined from the double KWW fit is good.

The value of the fast relaxation time τ_f decreases slightly (at all scattering angles) as the polymer concentration increases. The fast mode is observed to be diffusive under all conditions (see below), yielding a cooperative diffusion coefficient D_c. In terms of diffusion, these results indicate that D_c rises weakly ($D_c \sim c^{0.2}$) with increasing concentration. Although this value is less than the one predicted[47] (0.75) from the scaling theory, this relaxation process is interpreted as a cooperative diffusion mode. The origin of the difference in the values of the exponent is probably due to the low molecular weight ($M \approx 50\,000$) of the sample used in this work. Weak concentration dependences of D_c can also be inferred from previous DLS studies[1,3] on semidilute PVA solutions (fairly low molecular weight samples were also used in these experiments).

The slow relaxation time τ_s increases strongly with concentration, and the concentration dependence of τ_s can be described by a power law ($\tau_s \sim c^{4.0\pm0.2}$) (see Figure 6). We may note that this concentration dependence is much stronger than that predicted in the framework of the reptation model[47] for the concentration dependence of the self-diffusion coefficient ($D_s \sim c^{-1.8}$) in semidilute solutions. The strong slowing down of the chain disengagement process in this study can probably be associated with enhanced association effects at higher concentrations. In a recent DLS study on aqueous poly(vinyl alcohol−vinyl acetate) copolymer solutions, Horkay et al.[11] observed a $\mathbf{q}^2$ dependence of the slow mode and the slow relaxation time scaled with concentration as $\tau_s \sim c^3$.

Characteristics of the Correlation Function in the Pregel Domain. In Figure 7, the normalized time

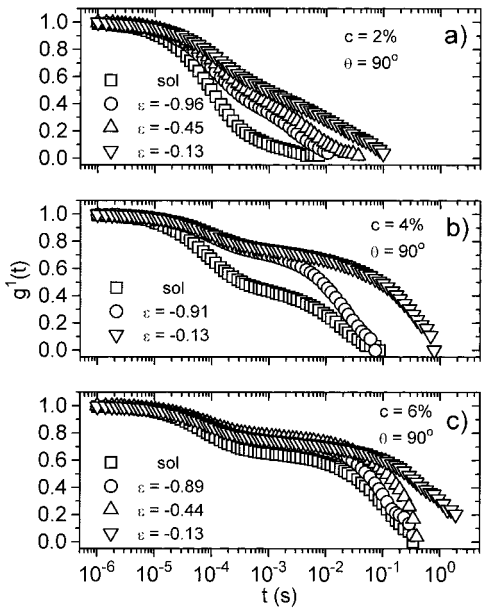

Figure 7. Evolution of the correlation functions at different stages of the gelation process for systems at the concentrations indicated.

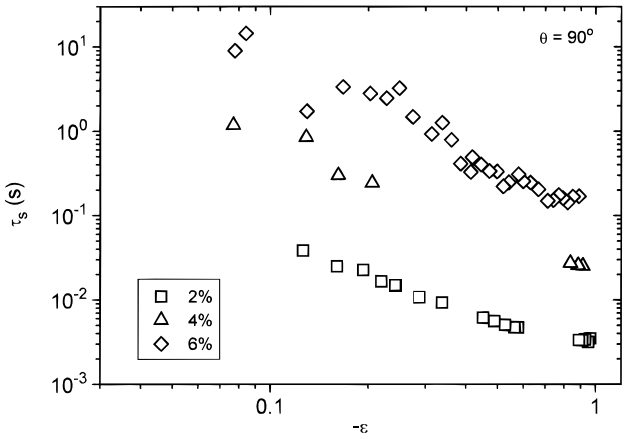

Figure 8. Variation of the slow relaxation time in the pregel zone for the concentrations indicated.

correlation data for different polymer concentrations at various stages in the pregel zone are depicted in the form of semilogarithmic plots. The parameter $\epsilon = (t - t_g)/t_g$ (t_g is the time of gelation) indicates the relative distance from the gel point. A close comparison of the correlation functions at a given value of ϵ reveals that the shift toward longer times increases as the concentration of the polymer increases. This tendency can probably be ascribed to enhanced entanglement effects with increasing concentration. A quantitative illustration of the changes of the slow relaxation time with ϵ and concentration is displayed in Figure 8. These results reveal that the slow relaxation process is slowed down as the cross-linking reaction proceeds and this trend becomes more pronounced as the polymer concentration increases.

Figure 9a−c shows the angular dependence of the time correlation functions at different gelation stages for a PVA concentration of 4% (w/w). The inset plots clearly demonstrate a stronger **q** dependence of the slow mode when the gel zone is approached. The **q** dependences of the slow mode at various conditions of gelation and polymer concentration are summarized in Figure 10. The most notable feature is that the inverse slow relaxation time for the low-concentration samples ex-

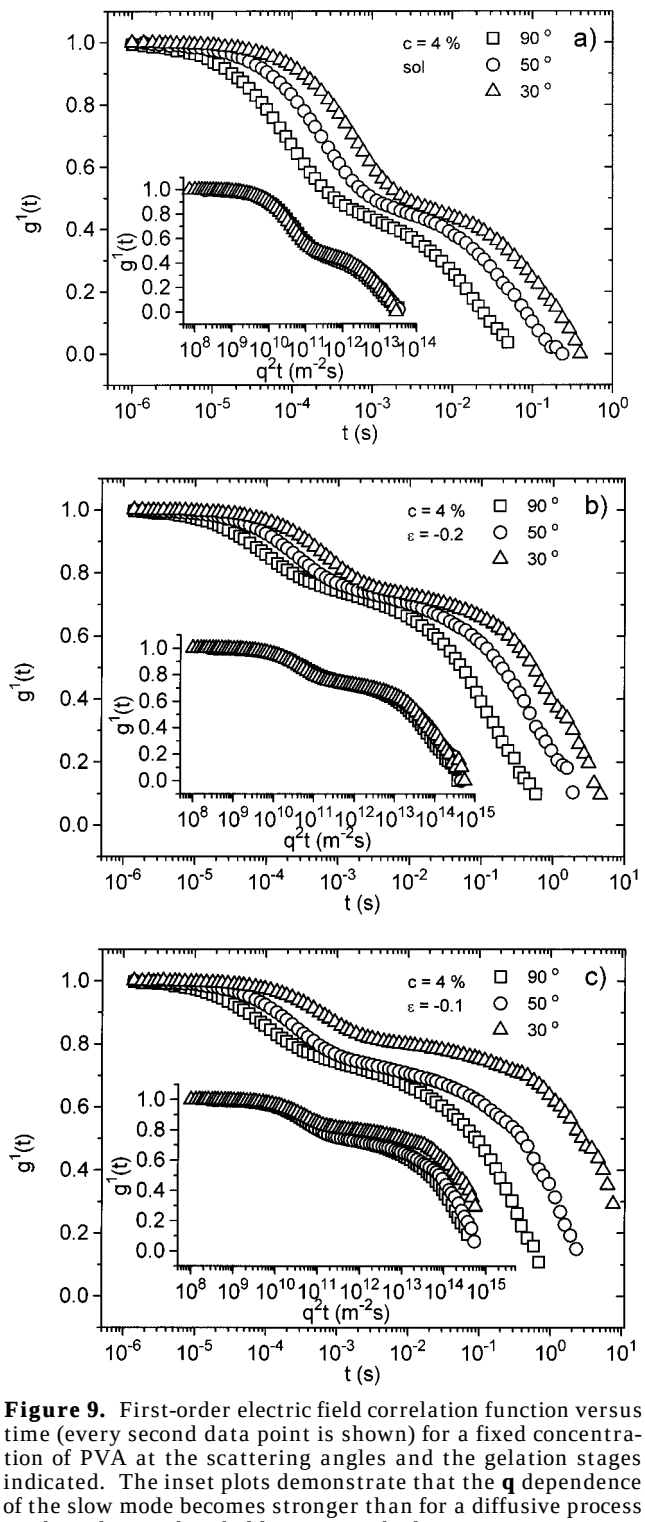

Figure 9. First-order electric field correlation function versus time (every second data point is shown) for a fixed concentration of PVA at the scattering angles and the gelation stages indicated. The inset plots demonstrate that the **q** dependence of the slow mode becomes stronger than for a diffusive process as the gelation threshold is approached.

hibits a strong **q** dependence when the gelation threshold is approached, while at higher concentrations this effect gradually disappears and the slow mode becomes practically diffusive in the whole pregel domain. This behavior can probably be rationalized in terms of changed heterogeneities of the network during the gelation process. It is generally expected[13,14,16] that the heterogeneities of the cluster size distribution become larger when the gelation threshold is approached. These results seem to indicate that incipient gels formed from systems of low polymer concentration become more heterogeneous than their corresponding solutions, while for systems of higher polymer concentration the non-

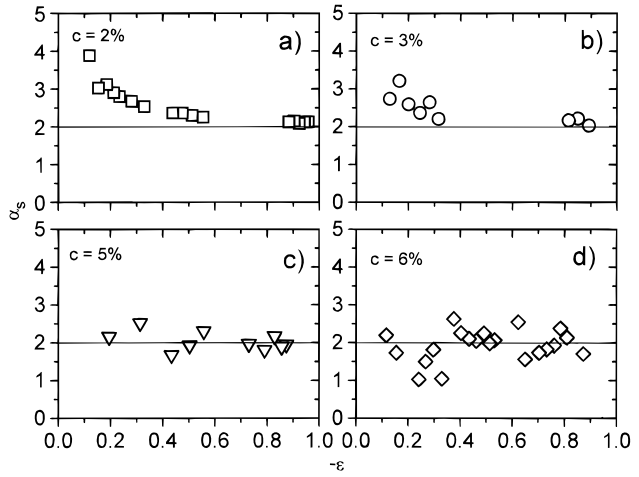

Figure 10. Power law exponent α, illustrating the **q** dependence of the inverse slow relaxation time as a function of the gelation state parameter ϵ, for the concentrations of PVA indicated.

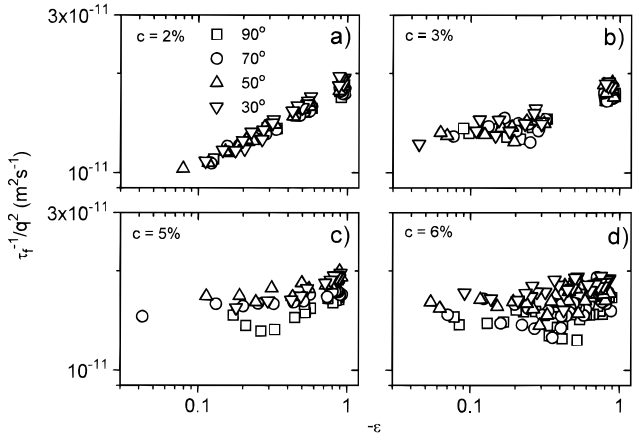

Figure 11. Variations of the cooperative diffusion coefficient as a function of ϵ for the scattering angles and concentrations indicated.

uniformities of the network is practically the same for the solution and the corresponding incipient gel. In this case the slow mode is diffusive. Several DLS studies[1,3,7,9,11] on PVA systems have reported a $\mathbf{q}^2$ dependence of the slow mode.

The variations of the quantity $\tau_f^{-1}/\mathbf{q}^2$ ($\tau_f^{-1} = D_c\mathbf{q}^2$) as a function of ϵ are depicted for different concentrations in Figure 11. At low polymer concentrations, the cooperative diffusion coefficient decreases as the gelation threshold is approached, while at higher concentrations D_c is practically independent of the stage of gelation. These features can probably also be associated with nonuniformities of the network. In a recent study,[48] the diffusion behavior in gels and the corresponding solutions was analyzed and it was found that nonuniformities in the network structure play an important role for the diffusion properties. Depending on the magnitude of these nonuniformities, the cooperative diffusion coefficient of the gel may be smaller than, equal to, or greater than the corresponding value of the solution. This model predicts a reduction of the diffusion coefficient for a gelling system with increasing nonuniformity of the network. In the light of this model, the present diffusion results (see Figure 11) for the low concentrations suggest that the nonuniformities of the networks increase when the gelation threshold is approached, while for the higher concentrations the structural nonuniformities are not significantly affected by the cross-linking reaction.

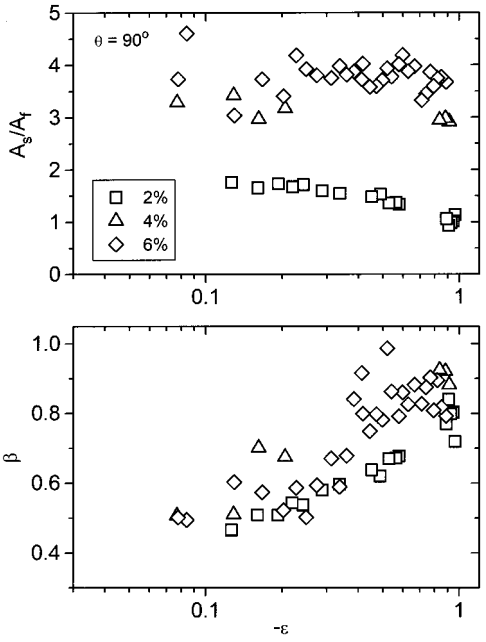

Figure 12. A_s/A_f and β as a function of ϵ for the scattering angle and the concentrations indicated.

The variations of the ratio A_s/A_f and the stretched exponent β as a function of ϵ are depicted in Figure 12. The ratio increases with increasing concentration. The value of the ratio is practically independent of the state of gelation for the higher concentrations, while for the system of low polymer concentration the slow mode becomes gradually more dominant as the gelation process proceeds. The general trend of the stretched exponent is that the value of β decreases as the gelation threshold is approached, indicating a broader distribution of relaxation times.

Characteristics of the Correlation Function at the Gel Point and in the Postgel Domain. By checking the dependence of the decay curves of the time correlation function on the scattering position of the incident light in the sample, no nonergodic features could be revealed for the above discussed pregel systems. However, at the gel point and in the postgel domain all systems displayed nonergodic features,[49−51] implying that the time-averaged intensity correlation function is not equal to the ensemble-averaged intensity correlation function. This indicates that the systems contain large-scale, stationary nonuniformities, so that the detection mode becomes heterodyned, with a resulting intensity correlation function given by[49,52]

$$g^{(2)}(\mathbf{q},t) = 1 + B[2R(1 - R)g^{(1)}(\mathbf{q},t) + R^2g^{(1)}(\mathbf{q},t)^2] \quad (4)$$

where R is the homodyne percentage, estimated with $g^{(1)}(\mathbf{q},t)|_{t=0} = 1$ and (1 − R) is the heterodyne percentage.

A consequence of the nonergodic effect is the reduction of the initial amplitude of the intensity autocorrelation function observed at the gelation threshold and in the postgel zone for the systems displayed in Figure 13. This reduction seems to be more pronounced as the polymer concentration increases. When the systems are in the sol state, the decay of the correlation function can always be described by a double KWW-stretched exponential function (see eq 2). For PVA−glutaraldehyde systems in close proximity to the gelation threshold, the initial decay of the correlation function exhibits ap-

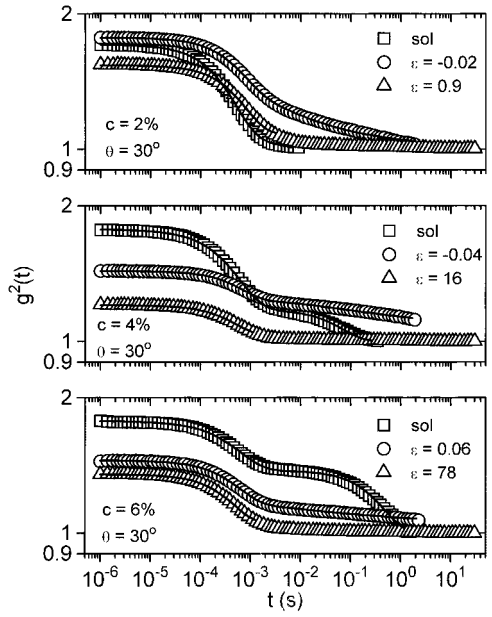

Figure 13. Measured intensity autocorrelation function versus time (every third data point is shown) at different stages during the gelation process and for the scattering angle and concentrations indicated.

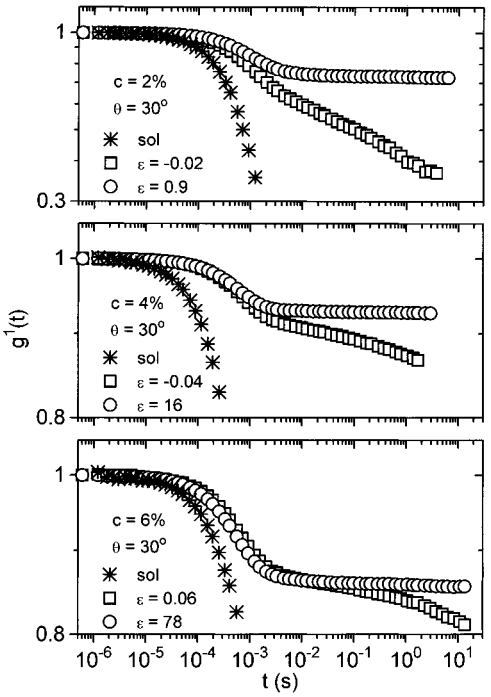

Figure 14. Plot of the first-order electric field correlation function, evaluated by means of eq 4, versus time (every third data point is shown) at different stages during the gelation process and for the scattering angle and concentrations indicated.

proximately an exponential profile, followed at longer times by a power law, a functional form that is intrinsically scale-invariant.[17] The solid curves, representing the incipient gels, have been fitted with the aid of a relationship of the same type as eq 1 in ref 16. This fractal time behavior[53] at longer times is a characteristic feature of processes that do not have a characteristic time scale. The power law behavior of the correlation function observed for the present incipient gels at longer times has also been reported for a number of incipient gels of various natures.[13,14,16,17,19,22,23,27,30−32,40] The analysis of the **q** dependence of the correlation function data at the gelation threshold reveals that the fast mode is diffusive for all systems, while the **q** dependence of the power law mode is more complex.

In the postgel domain, the slow mode is absent at all concentrations and the decay of the correlation function can be described by a single exponential (see Figure 13). The present DLS results on PVA systems at various stages of gelation suggest that the motions of clusters of various sizes give rise to the appearance of the slow relaxation mode, which is associated with inhomogeneities of the systems. In the postgel zone, the clusters will be trapped by the polymer networks and become parts of the gel networks. In this case, the clusters will not be able to drift and as a consequence the slow mode of the correlation function should disappear. The appearance of a single mode in the postgel domain has been reported for similar PVA gels[1,3,11] as well as for other types of gel.[22,26]

Another illustration of the nonergodic features of PVA of different concentrations is displayed in Figure 14, where the first-order electric field correlation function has been constructed with the aid of eq 4. Evidently the correlation functions for systems close to the gel point and for systems in the postgel regime decay to a nonzero value, implying that a fraction of the density fluctuations becomes frozen-in. An interesting finding in Figure 14 is that the separation between the long-time tales of the correlation functions for the incipient gel and the corresponding postgel is reduced as the polymer concentration of the system is increased. These results indicate that a relative larger fraction of the density fluctuations becomes frozen-in in the transition from the incipient gel to the postgel zone when the polymer concentration of the gelling system is low. This behavior may be rationalized in the following way. At a low concentration (2% w/w), the frozen-in effect is not important when the incipient gel is formed (see Figure 13), but as the cross-linking reaction proceeds, a larger fraction of the fluctuations in the pregel domain is frozen-in. At higher concentrations the entanglement effect gives rise to frozen structures already at the gelation threshold, and the contribution from cross-links during the reaction in the postgel zone does not seem to significantly change the frozen-in situation.

Summary and Conclusions

Dynamic light scattering measurements have been carried out on aqueous PVA solutions and on gelling solutions in the presence of a constant amount of cross-linker agent. In the solutions, two relaxation modes appeared and the slow mode became more dominant as the concentration increased. The stretched exponent β increased with polymer concentration, indicating that the solution became more homogeneous at higher concentrations. The fast mode is always diffusive, while the slow mode exhibits a somewhat stronger **q** dependence at low concentrations. A strong concentration dependence of the slow relaxation time, in the form of a power law ($\tau_s \sim c^4$), was observed in the semidilute regime.

In the pregel domain, the slow mode was diffusive for systems of higher polymer concentrations, while at lower concentrations, a much stronger **q** dependence of the slow mode was found as the gelation threshold was approached. The cooperative diffusion coefficient, evaluated from the fast relaxation mode, for systems of low polymer concentration decreased during the gelation process, while in systems of high concentration, D_c was

virtually constant in the pregel zone. These findings suggest that incipient gels formed from systems of low polymer concentration become more heterogeneous than their corresponding solutions. In systems of higher polymer concentration, the nonuniformities of the network are practically the same for the solutions and their corresponding incipient gels.

In close proximity to the gelation threshold, a slow mode in the form of a power law emerged, indicating a fractal time set in the scattered field. Beyond the gel point, the slow mode was absent and the decay of the correlation function could be described by a single exponential. Close to the gel point and in the postgel domain, fractions of the density fluctuations are frozen-in and the systems exhibited nonergodic features.

References and Notes

(1) Fang, L.; Brown, W. *Macromolecules* **1990**, *23*, 3284; **1992**, *25*, 6897.
(2) Geissler, E.; Horkay, F.; Hecht, A.-M. *Macromolecules* **1991**, *24*, 6006.
(3) Horkay, F.; Burchard, W.; Geissler, E.; Hecht, A.-M. *Macromolecules* **1993**, *26*, 1296.
(4) Horkay, F.; Burchard, W.; Geissler, E.; Hecht, A.-M.; Zrinyi, M. *Macromol. Chem., Macromol. Symp.* **1993**, *76*, 145.
(5) Horkay, F.; Hecht, A.-M.; Geissler, E. *Macromolecules* **1994**, *27*, 1795.
(6) McKenna, G.; Horkay, F. *Polymer* **1994**, *35*, 5737.
(7) Koike, A.; Nemoto, N.; Inoue, T.; Osaki, K. *Macromolecules* **1995**, *28*, 2339.
(8) Nemoto, N.; Koike, A.; Osaki, K. *Macromolecules* **1996**, *29*, 1445.
(9) Ikkai, F.; Shibayama, M.; Nomura, S.; Han, C. C. *J. Polym. Sci., Polym. Phys. Ed.* **1996**, *34*, 939.
(10) Wu, W.; Shibayama, M.; Roy, S.; Kurokawa, H.; Coyne, L. D.; Nomura, S.; Stein, R. S. *Macromolecules* **1990**, *23*, 2245.
(11) Horkay, F.; Burchard, W.; Hecht, A.-M.; Geissler, E. *Macromolecules* **1993**, *26*, 3375.
(12) Siegert, A. J. F. Massachusetts Institute of Technology, Radiation Laboratory Report No. 465, 1943.
(13) Martin, J. E.; Wilcoxon, J. P. *Phys. Rev. Lett.* **1988**, *61*, 373.
(14) Adam, M.; Delsanti, M.; Munch, J. P.; Durand, D. *Phys. Rev. Lett.* **1988**, *61*, 706.
(15) Burchard, W. *Prog. Colloid Polym. Sci.* **1988**, *78*, 63.
(16) Martin, J. E.; Wilcoxon, J.; Odinek, J. *J. Phys. Rev. A* **1991**, *43*, 858.
(17) Martin, J. E.; Adolf, D. *Annu. Rev. Phys. Chem.* **1991**, *42*, 311.
(18) Borsali, R.; Durand, D.; Fischer, E. W.; Giebel, L.; Busnel, J. P. *Polym. Networks Blends* **1991**, *1*, 11.
(19) Lang, P.; Burchard, W. *Macromolecules* **1991**, *24*, 814.
(20) Nyström, B.; Roots, J.; Carlsson, A.; Lindman, B. *Polymer* **1992**, *33*, 2875.
(21) Richtering, W.; Gleim, W.; Burchard, W. *Macromolecules* **1992**, *25*, 3795.
(22) Cotts, P. M. In *Synthesis, Characterization, and Theory of Polymeric Networks and Gels*; Aharoni, S. M., Ed.; Plenum Press: New York, 1992.
(23) Ren, S. Z.; Shi, W. F.; Zhang, W. B.; Sorensen, C. M. *Phys. Rev. A* **1992**, *45*, 2416.
(24) Hodgson, D. F.; Yu, Q.; Amis, E. J. In *Synthesis, Characterization, and Theory of Polymeric Networks and Gels*; Aharoni, S. M., Ed.; Plenum Press: New York, 1992.
(25) Tartaglia, P.; Rouch, J.; Chen, S. H. *Phys. Rev. A.* **1992**, *45*, 7257.
(26) Suzuki, Y.; Nozaki, K.; Yamamoto, T.; Itoh, K.; Nishio, I. *J. Chem. Phys.* **1992**, *97*, 3808.
(27) Burchard, W.; Lang, P.; Schulz, L.; Coviello, T. *Macromol. Chem. Symp.* **1992**, *58*, 21.
(28) Wang, C. H.; Zhang, X. Q. *Macromolecules*, **1993**, *26*, 707; **1995**, *28*, 2288.
(29) Nyström, B.; Walderhaug, H.; Hansen, F. K. *J. Phys. Chem.* **1993**, *97*, 7743.
(30) Ren, S. Z.; Sorensen, C. M. *Phys. Rev. Lett.* **1993**, *70*, 1727.
(31) Bauer, J.; Burchard, W. *Makromol. Chem., Macromol. Symp.* **1993**, *76*, 183.
(32) Konák, C.; Bansil, R. *Il Nuovo Cimento* **1994**, *16D*, 689.
(33) Nyström, B.; Thuresson, K.; Lindman, B. *Langmuir* **1995**, *11*, 1994.
(34) Fisken, B. J.; Ferri, F.; Cannell, D. S. *Phys. Rev. E* **1995**, *51*, 5922.
(35) Johannsson, R.; Chassenieux, C.; Durand, D.; Nicolai, T.; Vanhoorne, P.; Jérôme, R. *Macromolecules* **1995**, *28*, 8504.
(36) Nyström, B.; Lindman, B. *Macromolecules* **1995**, *28*, 967.
(37) Fuchs, T.; Richtering, W.; Burchard, W. *Macromol. Chem., Macromol. Symp.* **1995**, *99*, 227.
(38) Lairez, D.; Adam, M.; Raspaud, E.; Carton, J.-P.; Bouchaud, J.-P. *Macromol. Chem., Macromol. Symp.* **1995**, *90*, 203.
(39) Buhler, E.; Munch, J. P.; Candau, S. J. *J. Phys. II Fr.* **1995**, *5*, 765.
(40) Koike, A.; Nemoto, N.; Doi, E. *Polymer* **1996**, *37*, 587.
(41) Galinski, G.; Burchard, W. *Macromolecules* **1996**, *29*, 1498.
(42) Kohlrausch, R. *Pogg. Ann.* **1847**, *12* (3), 353.
(43) Williams, G.; Watts, D. C. *Trans. Faraday Soc.* **1970**, *66*, 80.
(44) Matthiez, P.; Mouttet, G.; Weissbuch, G. *J. Phys. (Paris)* **1980**, *41*, 519.
(45) Balsara, N. P.; Stepanek, P.; Lodge, T. P.; Tirell, M. *Macromolecules* **1991**, *24*, 6227.
(46) Provencher, S. W. *Makromol. Chem.* **1979**, *180*, 201.
(47) De Gennes, P.-G. *Scaling Concepts in Polymer Physics*; Cornell University Press: Ithaca, NY, 1979.
(48) Hecht, A.-M.; Guillermo, A.; Horkay, F.; Mallam, S.; Legrand, J. F.; Geissler, E. *Macromolecules* **1992**, *25*, 3677.
(49) Pusey, P. N.; van Megen, W. *Physica A* **1989**, *157*, 705.
(50) Joosten, J. G. H.; Geladé, E. T. F.; Pusey, P. N. *Phys. Rev. A* **1990**, *42*, 2161.
(51) Joosten, J. G. H.; McCarthy, J. L.; Pusey, P. N. *Macromolecules* **1991**, *24*, 6690.
(52) Geissler, E. In *Dynamic Light Scattering, the Method and Some Applications*; Brown, W., Ed.; Oxford University Press: Oxford, England, 1993.
(53) Shlesinger, M. F. *Annu. Rev. Phys. Chem.* **1988**, *39*, 269.

MA960705E